GENERALIZED FORWARD/BACKWARD SUBAPERTURE SMOOTHING TECHNIQUES FOR SAMPLE STARVED STAP

S. U. Pillai
Dept. of Electrical Engg.
Polytechnic University
Six Metrotech Center
Brooklyn, NY 11201

J. R. Guerci
Air Defense Technology
SAIC, Suite 400
4001 N. Fairfax Drive
Arlington, VA 22203

Y. L. Kim
Dept. of Electrical Engg.
Polytechnic University
Six Metrotech Center
Brooklyn, NY 11201

ABSTRACT

A major issue in space-time adaptive processing (STAP) for airborne moving target indicator (MTI) radar is the so-called sample support problem. Often, the available sample support for estimating the interference covariance matrix leads to severe rank deficiency, thereby precluding STAP beamforming based on the direct sample matrix inversion (SMI) method. The intrinsic interference subspace removal (ISR) technique, which is a computationally useful form of diagonally loaded SMI method, can handle this case, although the performance is poor in low sample situations. In this context, new subarray-subpulse schemes using forward and backward data vectors are introduced to overcome the data deficiency problem. It is shown here that multiplicative improvement in data samples can be obtained at the expense of negligible loss in space-time aperture of the steering vector.

1. INTRODUCTION

A major issue in space-time adaptive processing (STAP) for airborne moving target indicator (MTI) radar is the sample support problem. In this context, consider the radar scenario where the returned space-time snapshot signal may consist of a target echo and interferences such as jammer, clutter and thermal noise given by

$$\mathbf{x}_i = \alpha_t \mathbf{a}_t + \mathbf{c}_i \,, \tag{1}$$

where α_t and $\mathbf{a}_t \triangleq \mathbf{a}(\theta_t, \omega_{d_t})$ are the complex attenuation factor and target steering vector respectively associated with the spatial and doppler parameters θ_t and ω_{d_t} of the moving target, and $\mathbf{c}_i$ represents the total interference signal. Here $\mathbf{x}_i \in C^{MN}$ represents the concatenated space-time data vector formed from the array output vectors corresponding to the M pulse returns in a coherent processing interval (CPI) with interpulse interval T. Thus using N antenna elements, if $x_k(t_i)$ represents the k-th sensor output at $t = t_i$, then

$$\mathbf{x}(t_i) \triangleq [x_1(t_i), x_2(t_i), \cdots, x_N(t_i)] \tag{2}$$

and

$$\mathbf{x}_i \triangleq [\mathbf{x}(t_i), \mathbf{x}(t_i + T), \cdots, \mathbf{x}(t_i + (M-1)T)]^T \tag{3}$$

represent the array output and space-time snapshot data vectors, respectively. In the point-doppler estimation problem the optimum weight vector $\mathbf{w}_o$ is given by [4]

$$\mathbf{w}_o = R^{-1}\mathbf{a}_t \,, \tag{4}$$

where $R = E\{\mathbf{c}_i \mathbf{c}_i^*\}$ is the total interference matrix. For a uniform linear array with interelement spacing equal to d, the spatio-temporal steering vector can be expressed as $\mathbf{a}_t = \mathbf{a}(\theta, \omega_d) \triangleq \mathbf{b}_M(\omega_d) \otimes \mathbf{a}_N(\theta)$, where $\otimes$ represents the Kronecker product, and [4]

$$\mathbf{a}_N(\theta) \triangleq \left[1, e^{-j\pi d \sin\theta}, \cdots, e^{-j(N-1)\pi d \sin\theta}\right]^T \tag{5}$$

$$\mathbf{b}_M(\omega_d) \triangleq \left[1, e^{-j2\pi\omega_d}, \cdots, e^{-j2\pi(M-1)\omega_d}\right]^T \tag{6}$$

represent the spatial and temporal "steering vectors" respectively. Thus if the interference signal is assumed to be returns from a large number of independent scatterers, then

$$\mathbf{c}_i = \sum_{k=1}^{K} \alpha_k(i) \mathbf{b}_M(\omega_{d_k}) \otimes \mathbf{a}_N(\theta_k) + \mathbf{n}_i \tag{7}$$

and the total interference covariance matrix has the form

$$R = \sum_{k=1}^{K} P_k \mathbf{a}_k \mathbf{a}_k^* + \sigma^2 I_{MN} \,, \tag{8}$$

where $\mathbf{a}_k \triangleq \mathbf{b}_M(\omega_{d_k}) \otimes \mathbf{a}_N(\theta_k)$, and I_{MN} represents the identity matrix of size $MN \times MN$. Notice that clutter

This research was partially supported by the Office of Naval Research under contract N-00014-89-J-1512P-5.

doppler ω_k is linearly dependent on the bin location azimuth parameter $\sin\theta_k$ [4]. Here $\mathbf{n}_i$ represents thermal noise that is assumed to be uncorrelated and identically distributed among sensors and pulses. In actual practice, the interference covariance matrix R must be estimated by making use of the returns from neighboring range bins to the point of interest. This is most commonly accomplished with the formation of a sample covariance estimate given by

$$\hat{R} = \frac{1}{k}\sum_{j=1}^{k}\mathbf{x}_j\mathbf{x}_j^* = \frac{1}{k}Y_kY_k^*\,, \tag{9}$$

where

$$Y_k \stackrel{\triangle}{=} [\mathbf{x}_1, \mathbf{x}_2, \cdots, \mathbf{x}_k]\,. \tag{10}$$

Unfortunately, for the above procedure to work it is necessary to assume stationarity of the clutter over all range bins used in (9). Moreover since the size of R is large, (9) requires a very large number of range bins ($k > MN$) to guarantee a good estimate $\hat{R}$ that is nonsingular, and that much data may not be available in practice. Thus nonstationarity of the clutter together with insufficient data support to obtain nonsingular estimates makes the problem of clutter covariance matrix estimation open to other considerations.

Alternatively, since the optimal weight vector in (4) can be expressed as the net quiescent steering vector $\mathbf{a}_t$ that is free of all clutter subspace components, it has been shown that this idea can be implemented implicitly also in the sample starved situation by making use of the Hung-Turner projection [2, 3]. In fact with

$$\Phi_k = I_{MN} - Y_k(Y_k^*Y_k)^{-1}Y_k^*\,, \tag{11}$$

the weight vector

$$\mathbf{w}_{\mathrm{ISR}} = \Phi_k\mathbf{a}_t \tag{12}$$

retains the same structural properties of the optimal weight vector in (4) [3], and its performance in terms of SINR is optimum when the number of data samples used are equal to [1, 5]

$$k_{\mathrm{opt}} = \sqrt{(MN+1)r} - 1\,. \tag{13}$$

For example, for a 14 element array with 16 pulses, (13) gives the number of desired samples in this case to be about 80, (see Fig.1 traditional forward-only curve) provided we assume the clutter subspace rank r to be about 30 as in the Mountain-top data set [4]. Thus in this case, for peak performance we need about 80 samples, and it is desirable that this requirement on data samples be relaxed.

2. FORWARD/BACKWARD SUBSTRUCTURE METHODS FOR EXTENDED SAMPLE SUPPORT

2.1. Temporal Subpulse Method

The small sample size problem can be overcome to a great extent by exploiting the space-time structure of the steering vector together with the uncorrelated nature of the components of the interference covariance matrix. Towards this, let $\mathbf{x}_{i,j}^f$ represent the j-th forward subvector generated using J consecutive pulses in (3); Thus, for $j = 1, 2, \cdots, M-J+1$, define

$$\begin{aligned}\mathbf{x}_{i,j}^f \;\; &\stackrel{\triangle}{=}\;\; [\mathbf{x}(t_i+(j-1)T)\,,\, \mathbf{x}(t_i+jT)\,,\, \cdots \\ &\qquad \cdots\,,\, \mathbf{x}(t_i+(j+J-1)T)]^T\,.\end{aligned} \tag{14}$$

It is easy to show that the covariance matrix of the subvector in (14) can be expressed as

$$R_p^f = \sum_{k=1}^{K} P_k\mathbf{a}_p(k)\mathbf{a}_p^*(k)\,, \tag{15}$$

where $\mathbf{a}_p(k) \stackrel{\triangle}{=} \mathbf{b}_J(\omega_{d_k}) \otimes \mathbf{a}_N(\theta_k)$ with $\mathbf{b}_J(\omega_{d_k})$ representing the top $J\times 1$ subvector of $\mathbf{b}_M(\omega_{d_k})$. Notice that in an uncorrelated interference scene R_p^f is independent of j and i, so that the data vectors in (14) can be separately used to generate the sample data matrix. Thus with

$$Y_j^f \stackrel{\triangle}{=} [\mathbf{x}_{1,j}^f, \mathbf{x}_{2,j}^f, \cdots, \mathbf{x}_{k,j}^f]\,, \tag{16}$$

we have the extended data matrix

$$Y^f = [Y_1^f, Y_2^f, \cdots, Y_{M-J+1}^f]\,. \tag{17}$$

Notice that although Y^f corresponds to only J pulses, it has an effective sample support size of $(M-J+1)k$, which could be large compared to k.

The uncorrelated nature of the interference data together with the uniform array can be further exploited to generate backward data matrices. Towards this, let $\mathbf{x}_{i,j}^b$ represent the complex conjugated and reversed data vector in (14). Then with the backward data vector

$$\mathbf{x}^b(t_i) \stackrel{\triangle}{=} [x_N^*(t_i), x_{N-1}^*(t_i), \cdots, x_1^*(t_i)]\,, \tag{18}$$

we have

$$\begin{aligned}\mathbf{x}_{i,j}^b &= \big[\mathbf{x}^b(t_i+(j+J-1)T)\,,\, \cdots\,, \\ &\qquad \cdots\,,\, \mathbf{x}^b(t_i+jT)\,,\, \mathbf{x}^b(t_i+(j-1)T)\big]^T\,.\end{aligned} \tag{19}$$

Once again, exploiting the uncorrelated nature of the scatterers it is easy to see that the covariance matrix R_p^b for (19) has the same form as in (15) and hence, we may define Y^b as in (16)–(17). Thus

$$Y^b = [Y_1^b, Y_2^b, \cdots Y_{M-J+1}^b]\,, \tag{20}$$

where $Y_j^b = [\mathbf{x}_{1,j}^b, \mathbf{x}_{2,j}^b, \cdots, \mathbf{x}_{k,j}^b]$. Finally

$$Y_p^{f/b} = [Y^f \,|\, Y^b] \tag{21}$$

gives the generalized forward/backward expanded data matrix of size $JM\times 2(M-J+1)k$, each column of which have the same ensemble averaged covariance matrix. Notice that the effective sample size in $Y_p^{f/b}$ has gone up by a factor of $2(M-J+1)$, whereas the effective pulse length has been reduced from M to J. Thus, for example, if J is chosen to be $M-1$, the number of pulses are reduced by unity, whereas the effective data goes up by a factor of four! This is a remarkable achievement considering that the performance degradation in the doppler domain due to loss of one pulse, is insignificant compared to the sample data improvement factor of four. Fig.1 shows the results of simulation using the proposed subpulse method with $J=M-1$, for the f/b case in terms of the SINR loss with details as shown there. Notice that with $J=M-1$, effective data goes up by a factor of four, and the peak performance is attained with 20 actual samples. The multiplication factor of four makes the effective number of samples to be 80 and this is consistent with the discussion that follows (13).

2.2. Spatial Subarray Method

Alternatively, the freedom present in the spatial domain can be explored to define similar forward and backward subvectors. Towards this, let

$$\mathbf{z}_l^f(t_i) = [x_l(t_i), x_{l+1}(t_i), \cdots, x_{l+L-1}(t_i)]\,, \qquad l = 1 \to N-L+1 \tag{22}$$

represent the l-th forward subarray of size L generated from the spatial vector $\mathbf{x}(t_i)$ in (2). Next define

$$\mathbf{z}_{i,l}^f = \left[\mathbf{z}_l^f(t_i), \mathbf{z}_l^f(t_i+T), \cdots, \mathbf{z}_l^f(t_i+(M-1)T)\right]^T \qquad l = 1 \to N-L+1\,, \quad i = 1 \to k \tag{23}$$

to be the concatenated data vector from M such pulses. Notice that $\mathbf{z}_{i,l}^f$ is of size $ML \times 1$, and its covariance matrix can be expressed as

$$R_s^f = \sum_{k=1}^{K} P_k \mathbf{a}_s(k)\mathbf{a}_s^*(k)\,, \tag{24}$$

$$\mathbf{a}_s(k) \triangleq \mathbf{b}_M(\omega_{d_k}) \otimes \mathbf{a}_L(\theta_k) \tag{25}$$

with $\mathbf{a}_L(\theta_k)$ representing the top $L \times 1$ subvector of $\mathbf{a}_N(\theta_k)$. R_s^f is also independent of l and i, implying that every data vector in (23) has the same covariance matrix. Once again proceeding as in the previous section, it can be shown that

$$Y_s^{f/b} = [Z^f \mid Z^b] \tag{26}$$

represents the "extended" data vector set in this case. Here $Z^f = [Z_1^f, Z_2^f, \cdots, Z_{N-L+1}^f]$ and $Z^b = [Z_1^b, Z_2^b, \cdots, Z_{N-L+1}^b]$ with $Z_l^f = [\mathbf{z}_{1,l}^f, \mathbf{z}_{2,l}^f, \cdots, \mathbf{z}_{k,l}^f]$, $l = 1 \to N-L+1$, and $Z_l^b = [\mathbf{z}_{1,l}^b, \mathbf{z}_{2,l}^b, \cdots, \mathbf{z}_{k,l}^b]$ and $\mathbf{z}_{i,l}^b = J_o(\mathbf{z}_{i,l}^f)^*$, where J_o represents the exchange matrix of size $ML \times ML$. Notice that $Y_s^{f/b}$ contains $2(N-L+1)k$ samples, although the array aperture only corresponds to L sensors. Thus, for example, if L is chosen to be $N-1$, then effective number of samples can be increased by a factor of four, whereas the antenna size gets reduced by one sensor element only. Once again this improvement in performance by a multiplication factor is very significant.

The temporal and spatial freedom present in the space-time data vector can be exploited simultaneously to even greater advantage in the data domain.

2.3. Subpulse-Subarray Method

To simultaneously exploit the spatial and temporal characteristics, with the l-th subarray as defined in (22), consider J such consecutive subarray vectors concatenated together to generate

$$\begin{aligned}\mathbf{w}_{l,j}^f(i) &= \Big[\mathbf{z}_l^f(t_i+(j-1)T), \mathbf{z}_l^f(t_i+jT), \cdots \\ &\qquad \cdots, \mathbf{z}_l^f(t_i+(j+J-1)T)\Big]^T\,,\end{aligned}$$

$$l = 1 \to N-L+1 \;\text{ and }\; j = 1 \to M-J+1\,. \tag{27}$$

$\mathbf{w}_{l,j}^f(i)$ is of size $JL \times 1$, and represent forward-data vectors. It is easy to show that the covariance matrix of the data vector in (27) can be expressed as

$$R_{p,s}^f \triangleq \sum_{k=1}^{k} P_k \mathbf{a}_{p,s}(k)\mathbf{a}_{p,s}^*(k) \tag{28}$$

where

$$\mathbf{a}_{p,s}(k) \triangleq \mathbf{b}_J(\omega_{d_k}) \otimes \mathbf{a}_L(\theta_k)\,. \tag{29}$$

Notice that (28) is independent of l, j and i, implying that all these data vectors have the same covariance matrix, and hence they may all be used in their estimation. Obviously the extension to the backward data case can be done in a similar manner. Thus proceeding as before, we obtain the total data matrix

$$Y_{p,s}^{f/b} = [W^f \mid W^b]\,, \tag{30}$$

where $W^f = [W_{1,1}^f, W_{1,2}^f, \cdots, W_{(M-J+1),(N-L+1)}^f]$ with $W_{i,j}^f = [\mathbf{w}_{i,j}^f(1), \mathbf{w}_{i,j}^f(2), \cdots, \mathbf{w}_{i,j}^f(k)]$ and $W^b = [W_{1,1}^b, W_{1,2}^b, \cdots, W_{(M-J+1),(N-L+1)}^b]$, where $W_{i,j}^b = J_o\left(W_{i,j}^f\right)^*$. Notice that $Y_{p,s}^{f/b}$ has $2(M-J+1)(N-L+1)k$ column vector each of size $JL \times 1$. Thus the effective data samples has increased by a factor of $2(M-J+1)(N-L+1)$, whereas the steering vector size has been reduced to $JL \times 1$.

Fig.1 also shows the results of simulation for the SINR loss using the subpulse-subarray method with $J = M-1$ and $L = N-1$ for the forward only as well as the forward/backward case. The effective data in this case goes up by a factor of 8 for the f/b case, and in fact as the solid curve in Fig.1 shows, ten actual samples are able to achieve the peak performance in the forward/backward case. Once again this is consistent with (13).

Fig.2 refers to the adaptive matched filter output for target detection for the forward-only as well as the f/b case. Comparisons are made between the traditional case (no subarrays or subpulses) and the subpulse case discussed in section 2.1. From Fig.1, since twenty actual samples realize peak performance in the f/b subpulse case, they are used to generate the corresponding weight vector and the output amplitude response $|\mathbf{w}^*\mathbf{x}|$. Notice that with 20 samples, only the generalized f/b subpulse case is able to detect the target (buried 50 dB below the clutter level and 10 dB above the noise floor) in an unambiguous fashion.

3. CONCLUSIONS

To overcome the small sample support problem in space-time adaptive processing in nonstationary environments, a generalized subaperture-subpulse method is introduced together with forward/backward processing. The structure of the actual space-time steering vector as well as the total interference covariance matrix plays a key role, and they are exploited to generate effective additional data vectors of reduced size. However the multiplicative performance gain in the available number of data vectors far outweighs the space-time aperture loss, and simulation results using actual mountain top data are presented to illustrate the usefulness of the proposed method. In essence, multiplicative improvement in data samples can be obtained at the expense of negligible loss in space-time aperture of the steering vector. This is rather remarkable considering that the aperture loss is only linear, whereas the sample support improvement is multiplicative by almost an order even in the simplest situation of this algorithm.

4. REFERENCES

[1] Gierull, C.H., "Performance Analysis of Fast Projections of the Hung-Turner Type for Adaptive Beamforming", *Signal Processing*, vol. 50, 1996.

[2] Hung, E.K.L., and Turner, R.M., "A Fast Beamforming Algorithm for Large Arrays", *IEEE Transactions on Aerospace and Electronic Systems*, vol. 19, no. 4, July 1983.

[3] Pillai, S.U., and Kim, Y.L., and Guerci, J.R., "New Techniques for Minimal Sample Support Space-Time Adaptive Radar", Under preparation.

[4] Ward, J., "Space-Time Adaptive Processing", Technical Report 1015, MIT Lincoln Laboratory, Lexington, MA, December 1994.

[5] Zatman, M., "Properties of Hung-Turner Projections and their Relationship to the Eigencanceller", *IEEE 30th Asilomar Conference on Signals, Systems and Computers*, Pacific Grove, CA 1996.

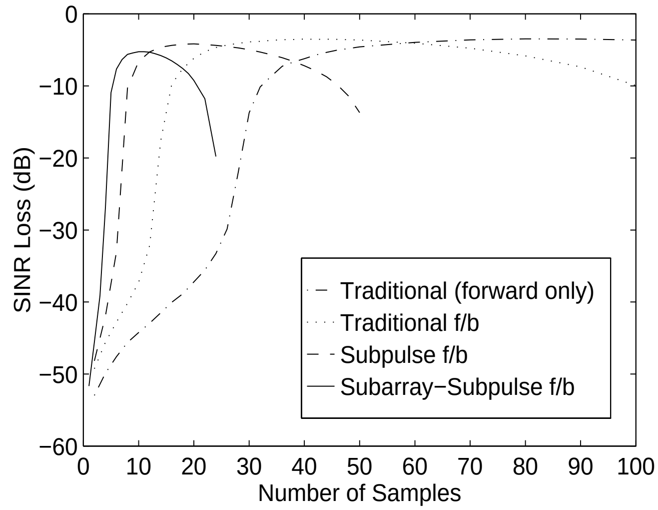

Figure 1: Forward/backward subpulse only and subarray-subpulse techniques for sample starved STAP. Two subvectors using fifteen consecutive pulses are generated in both forward and backward case.

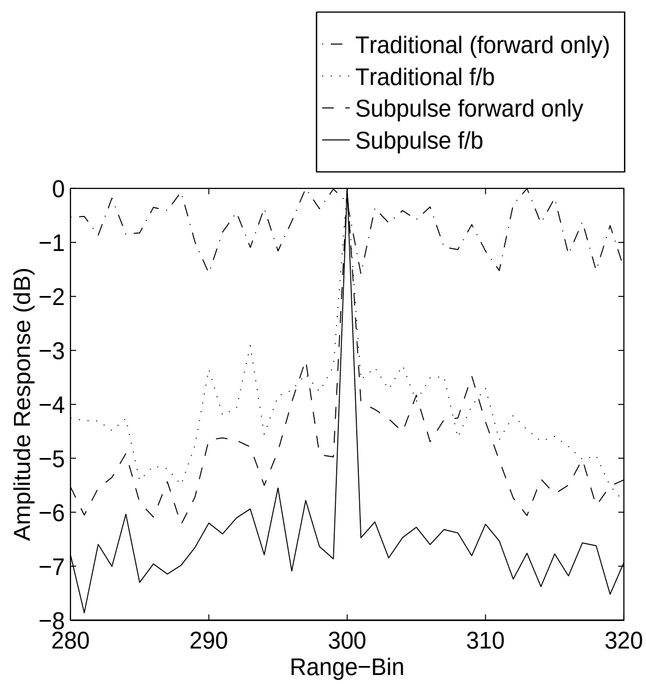

Figure 2: Subpulse vs Traditional Approach: Adaptive matched filter output for target detection. Twenty actual number of samples are used in this case (see Fig.1). Results of 100 independent simulation averages are shown here.